EISSN: 2707-0425

*East African Journal of Science, Technology and Innovation, Vol. 6 (4): September 2025*



# Performance Analysis of MIMO-OTFS with Advanced Detection Techniques for High-Mobility Wireless Communication

* [1]MAMADAPUR, P., [2]ANITHA S., [3]SENTHIL KUMARAN, T., [4]PILLAI, C. S. [5]ASHOK KUMAR, P. S.

[1]Research Scholar, ACS College of Engineering, Visvesveraya Technological University, Belagavi- 590018
[2]Research Supervisor, Professor, ACS College of Engineering, Visvesveraya Technological University, Belagavi- 590018
[3,4]Co supervisor, Professor, ACS College of Engineering, Visvesveraya Technological University, Belagavi- 590018
[5]Professor, ACS College of Engineering, Visvesveraya Technological University, Belagavi

*** Corresponding author:** panchaxari.m@gmail.com

**Abstract**

Orthogonal Frequency Division Multiplexing (OFDM) has been the dominant multicarrier transmission technique in wireless communication; however, its susceptibility to inter-carrier interference and Doppler spread limits reliability under high-mobility conditions. Orthogonal Time Frequency Space (OTFS) modulation, in contrast to conventional time–frequency domain schemes, transforms information symbols into the delay–Doppler (DD) domain via a symplectic finite Fourier transform. This enables the effective exploitation of the channel's inherent sparsity and enhancing robustness against doubly selective fading effects. Extending this framework, a Multiple-Input Multiple-Output (MIMO)-OTFS system is developed to enhance spatial diversity and throughput in rapidly varying propagation environments.

Specifically, this study investigates the Bit Error Rate (BER) performance of OTFS under the Extended Vehicular A (EVA) channel model. The results are benchmarked against conventional Orthogonal Frequency Division Multiplexing (OFDM) operating over a Rayleigh fading channel. The scope of the analysis is broadened to encompass MIMO-OTFS systems with 2×2 configuration, an Expectation Propagation (EP)-based detection strategy, and a Deep Learning (DL)-oriented detection framework.

The robustness of the MIMO-OTFS system is further substantiated through simulations conducted across diverse mobility conditions, with consistent performance observed even at vehicular velocities reaching 120 km/h. Additionally, this work examines the incorporation of Non-Orthogonal Multiple Access (NOMA) into the MIMO-OTFS framework. The MIMO-OTFS-NOMA configuration, particularly for users with favorable channel conditions (near users), exhibits exceptional BER performance. The SE versus SNR curves confirm that DL-aided MIMO-OTFS achieves the best trade-off between reliability and efficiency. Collectively, the results underscore the potential of MIMO-OTFS, as a highly resilient and spectrally efficient solution for next-generation wireless systems operating under severe channel time variability and mobility constraints.

***Key words:*** *BER; DL; EP; OTFS; Spectral Efficiency.*

**Cite as**: Mamadapur *et al.* (2025) Performance Analysis of MIMO-OTFS with Advanced Detection Techniques for High-Mobility Wireless Communication. *East African Journal of Science, Technology and Innovation, 6(4)*.

Received: 02/05/2025
Accepted: 01/09/2025
Published: 30/09/2025

## Introduction

The ongoing development of wireless communication technologies is motivated by the imperative to resolve the foundational issues linked with achieving higher data rates, enhanced spectral efficiency, and robust reliability in heterogeneous propagation environments. As we progress toward 6G communication systems, high-mobility scenarios pose significant challenges due to time-varying channel conditions and Doppler effects that severely impact conventional modulation schemes.

OTFS modulation has been recognized as a promising approach for addressing these challenges by exploiting the delay-Doppler (DD) domain for signal representation and processing. While conventional OTFS demonstrates notable advantages, opportunities for further enhancement of system performance, particularly through its integration with advanced methodologies such as MIMO architectures and intelligent detection algorithms. MIMO technology leverages spatial diversity and multiplexing to increase capacity and reliability, making MIMO-OTFS a particularly promising approach for next-generation wireless systems. Moreover, the integration of machine learning techniques particularly DL introduces promising avenues for enhancing detection efficiency and accuracy in complex MIMO-OTFS communication systems. This study presents an in-depth analysis of OTFS modulation and its enhanced variants, with particular focus on MIMO-OTFS implementations and advanced detection techniques. We begin by comparing the BER performance of OTFS and OFDM under EVA and Rayleigh channel models respectively, across various SNR values. We investigate the impact of user mobility on system performance. To address multi-user scenarios, we conduct a performance evaluation of MIMO-OTFS with NOMA, demonstrating its effectiveness in serving both near and far users simultaneously.

The progression of wireless communication systems has been characterized by ongoing innovations in modulation schemes to effectively meet evolving performance demands and overcome emerging channel impairments. Tse *et al.* (2005) established a rigorous theoretical framework for wireless communication, elucidating the core principles that form the basis of contemporary wireless system design and analysis. As mobile communications progressed from 3G to 4G, OFDM emerged as the dominant modulation technique due to its spectral efficiency and ability to combat frequency-selective fading through simple equalization techniques **(**Wu and Zou, 1995).

However Hlawatsch and Matz (2011), identified significant limitations of OFDM in high-mobility scenarios, where Doppler shifts cause inter-carrier interference (ICI) and degrade performance considerably. This limitation became increasingly important as applications requiring reliable communications in high-mobility environments, such as vehicle-to-vehicle (V2V) communications and high-speed trains gained prominence.

Orthogonal Time Frequency Space (OTFS) modulation was first conceptualized and introduced by Hadani *et al.* (2017) as a novel two-dimensional modulation technique that operates in the DD domain rather than the conventional TF domain. This groundbreaking approach leverages the quasi-stationarity of wireless channels in the DD domain, making it particularly suitable for high-mobility scenarios.

Raviteja *et al.* (2018) conducted an in depth investigation of OTFS modulation, highlighting its performance advantages over OFDM, particularly in channels characterized by high Doppler spread. Their study demonstrated that OTFS achieves substantial diversity gains by mapping each symbol across the entire TF domain, thereby ensuring resilient performance in highly dynamic and dispersive channel environments.

Wei *et al.* (2021) developed low-complexity detection algorithms for OTFS, addressing one of the primary challenges in practical implementation. The developed message-passing-based detection scheme significantly lowers computational complexity without substantial degradation in performance. This laid the ground work for exploring more advanced detection techniques in subsequent research.

MIMO systems, as described by Telatar E. (1999), exploit spatial diversity to increase reliability and capacity. The integration of MIMO technology with OTFS represents a natural evolution to further enhance system performance. Ramachandran and Chockalingam (2018) were among the first to investigate the integration of MIMO with OTFS, demonstrating that MIMO-OTFS architectures offer substantial performance improvements compared to their SISO-OTFS counterparts.

In recent years, the integration of machine learning techniques—especially DL into wireless communications has garnered considerable interest. Ye *et al.* (2017) presented a DL method for emphasizing its efficacy in improving signal detection and channel estimation tasks.

A low-complexity DL-based detector using a 2D convolutional neural network (2D-CNN) is proposed by Enku et. al. (2022) for MIMO-OTFS systems. The model efficiently learns the input-output relationship by leveraging the structure of the DD channel. A data augmentation strategy, based on a light-weight linear detector, further enhances detection performance. Unlike conventional DL detectors, the proposed model operates without explicit channel input, enabling robust learning under varying channel conditions. The simulation outcomes reveal that the proposed detector achieves enhanced performance relative to conventional OTFS detection techniques.

Surabhi *et al.* (2020) propose a low-complexity linear equalizers for OTFS system by leveraging the inherent organization of the effective DD channel matrix. This matrix exhibits a block circulant with circulant block structure, which can be leveraged to enable the design of computationally efficient equalizers

NOMA has gained recognition as an effective multiple access strategy for improving system capacity in multi-user communication environments. Ding *et al.* (2017) articulated the core concepts of NOMA, illustrating its capability to enhance spectral efficiency and promote user fairness within the context of 5G wireless networks. Ding *et al.* (2019), also proposed a NOMA-OTFS framework for multi-user communications in high-mobility environments. Their study showed that NOMA-OTFS is capable of efficiently supporting multiple users experiencing heterogeneous channel conditions by employing power allocation strategies based

on user proximity, thereby ensuring satisfactory performance across the user base.
The Pu *et al.* (2024) presents a low-complexity expectation propagation (EP) detector tailored for OTFS modulation with practical rectangular pulse shaping waveforms. The proposed approach exploits both the inherent sparsity and the block circulant structure of the effective channel covariance matrix in the delay-Doppler (DD) domain to substantially reduce the computational burden typically associated with EP-based detection. By systematically utilizing the unique structural properties of the OTFS channel, the detector efficiently approximates the marginal posterior distributions of the transmitted symbols. Extensive simulation results validate the efficacy of the proposed algorithm, demonstrating that it not only significantly lowers the computational complexity compared to conventional methods but also maintains robust detection performance across a wide range of signal-to-noise ratio (SNR) conditions.

The impact of user mobility on communication system performance is a critical consideration, particularly for applications such as vehicle-to-everything (V2X) communications and high-speed railway communications.
Although significant strides have been taken in OTFS and MIMO-OTFS technologies, several research gaps persist. First, while research efforts have concentrated on individual aspects of MIMO-OTFS performance, a comprehensive comparative analysis encompassing conventional OTFS, MIMO-OTFS with varying configurations, and advanced detection techniques under unified simulation settings remains absent in the existing literature. Second, the integration of deep learning (DL)-based detection with MIMO-OTFS, along with its performance implications across diverse mobility scenarios and spectral efficiency requirements, warrants further exploration.

This traces the evolution of OTFS technology from its foundational inception to advanced implementations integrating MIMO, NOMA, and deep learning (DL)-based detection techniques. It emphasizes the potential of these emerging technologies to enhance high-mobility wireless communication systems while delineating the research gaps that form the basis of this study. The comprehensive performance evaluation conducted in this work seeks to address these gaps, offering critical insights for the design and development of robust communication frameworks suited to future high-mobility wireless environments.

The organization of the remainder of this work is structured to present the following components in sequence. Materials and Methods**-** outlines the key aspects of the OTFS modulation principles, MIMO-OTFS framework and the various detection techniques considered, results-section presents a comprehensive performance evaluation of various detection algorithms in the MIMO-OTFS framework, with a particular focus on Bit Error Rate (BER) and spectral efficiency under high-mobility and multi-user scenarios, discussion- section discusses the results of the simulations.

## Materials and Methods

### *OFDM*

The input to the OFDM system consists of Quadrature Phase Shift Keying (QPSK) modulated symbols. These symbols are arranged in the frequency domain across N subcarriers, where N = 64.

$$X[k], \qquad k = 0,1, \dots \dots \dots N-1 \qquad (1)$$

These symbols are subsequently subjected to further processing operations, serial-to-parallel conversion to distribute them across multiple orthogonal subcarriers. The frequency-domain symbols are mapped onto the time domain using the Inverse Fast Fourier Transform (IFFT).

$$x[n] = \frac{1}{N}\sum_{k=0}^{N-1} X[k].e^{j2\pi kn/N}, n = 0,1,..N-1 \qquad (2)$$

A cyclic prefix (CP) is employed to reduce inter-symbol interference (ISI) induced by multipath propagation. This process entails extracting the last $L_{CP}$ samples from the IFFT output and prefixing them at the onset of the transmitted symbol, followed by parallel-to-serial conversion to produce the final time-domain signal for transmission.

$$x_{CP}[n] = \begin{cases} x[n+N-L_{CP}] \\ x[n] \end{cases} \qquad (3)$$

The final OFDM symbol consists of the time-domain signal with a prepended cyclic prefix. The total symbol length is N + $L_{CP}$, where $L_{CP}$ = 16 corresponds to the cyclic prefix duration in samples.

During the reception process, the reverse processing is initiated by performing a serial-to-parallel conversion of the incoming signal. Following this, the cyclic prefix is discarded prior to further processing to facilitate further signal processing, and a Fast Fourier Transform (FFT) is applied to transform the time-domain signal into its frequency-domain representation.

$$Y[k] = \sum_{n=0}^{N-1} y'[n]e^{-j2\pi kn/N}, \quad k = 0,1,.N-1 \qquad (4)$$

Rayleigh fading is predominantly adopted to emulate the wireless channel in OFDM simulations. The channel impulse response can be mathematically represented as follows:

$$h(\tau,t) = \sum_i \alpha_i(t)\delta(\tau-\tau_i) \qquad (5)$$

Here, $\alpha_i(t)$ refers to random variables following a statistically modeled complex Gaussian process with a mean of zero, while $\tau_i$ corresponds to the propagation delay related with the i-th multipath component.

The signal acquired at the receiver end is further affected by AWGN(Additive White Gaussian Noise), which represents random noise introduced by the transmission medium.

$$y[n] = \sum_{l=0}^{L-1} h[l]\, s[n-l] + w[n] \qquad (6)$$

Channel equalization is then performed to compensate for channel-induced distortions, typically through zero-forcing or MMSE techniques. The equalized symbols undergo parallel-to-serial conversion and QPSK demodulation is employed to retrieve the transmitted bit stream from the received signal.

***OTFS Modulation***

The OTFS modulation represents a paradigm shift in modulation technique that operates in the DD domain, offering superior resilience to high-mobility scenarios. The process begins with QPSK modulation of the input bit stream, resulting in complex symbols that are subsequently arranged in a two-dimensional DD grid. These symbols undergo a two-dimensional Inverse Symplectic Finite Fourier Transform (ISFFT), which comprises an Inverse Discrete Fourier Transform (IDFT) along the Doppler dimension followed by a

Discrete Fourier Transform (DFT) along the delay dimension. This transforms the DD representation into a TF grid

ISFFT Converts the symbols from delay-Doppler $X_{dd}$ to time-frequency domain $X_{tf}$

$$X_{tf}[m,n] = \frac{1}{\sqrt{MN}} \sum_{k=0}^{N-1} \sum_{i=0}^{M-1} X_{DD}[k,l] e^{j2\pi\left(\frac{nk}{N} - \frac{ml}{M}\right)} \quad (7)$$

The Heisenberg transform converts the transformed symbols $X_{tf}$ to a time-domain signal.

$$x(t) = \sum_{n=0}^{N-1} \sum_{m=0}^{M-1} X_{tf}[m,n] g_{tx}(t - nT) e^{-2j\pi m\Delta f(t-nT)} \quad (8)$$

At the receiver Wigner transform extracts the TF representation. A two-dimensional Symplectic Finite Fourier Transform (SFFT), consisting of a DFT along the time dimension and an IDFT along the frequency dimension, converts the signal back to the DD domain. Channel equalization is executed within this domain, in which the channel demonstrates a quasi-stationary response regardless of time variations, providing significant advantages over conventional TF domain processing. Finally, QPSK demodulation recovers the original information bits.

### *MIMO-OTFS System*

In the MIMO-OTFS system with $N_t$ transmit antennas and $N_r$ receive antenna, the signal received at the j-th receive antenna is

$$y_j(t) = \sum_{i=1}^{N_t} h_{ji}(t,\tau) * x_i(t) + n_j(t) \quad (9)$$

### *Channel Model*

We employ the EVA channel model, which is a standardized 3GPP channel model for vehicular environments. The EVA model includes multiple paths with specified delays and average power. EVA channel model is as shown in table 1 (Del *et al.*, 2012).

**Table 1**

*EVA Channel model*

| **Tap** | **1** | **2** | **3** | **4** | **5** | **6** | **7** | **8** | **9** |
|---|---|---|---|---|---|---|---|---|---|
| **Delay(ns)** | 0 | 30 | 150 | 310 | 370 | 710 | 1090 | 1730 | 2510 |
| **Relative Power(dB)** | 0.0 | -1.5 | -1.4 | -3.6 | -0.6 | -9.1 | -7.0 | -12.0 | -16.9 |

### *Detection Techniques*

Figure 1 illustrates the comprehensive architecture of the MIMO-OTFS communication system. In the transmitter section, the process commences with binary input data that undergoes QPSK modulation. The modulated signal components are thereafter subjected to a MIMO encoder that systematically distributes the data stream across multiple transmit antennas. Antenna-specific symbol mapping is performed onto the DD domain, followed by the application of a two-dimensional ISFFT. These signals subsequently traverse an EVA MIMO channel, which accurately models the challenging multipath fading conditions encountered in high-mobility wireless scenarios, with AWGN introduced at each receive antenna to simulate real-world impairments. At the receiver, each antenna's signal undergoes a two-dimensional Symplectic Finite Fourier Transform (SFFT). These symbols from multiple receive antennas are then collectively processed by the MIMO detector, which incorporates various detection algorithms of increasing sophistication—ZF, MMSE, EP, and DL—to effectively enhance detection reliability. The detected symbols finally undergo QPSK demodulation to recover the original binary data.

**Figure 1**

*MIMO OTFS Communication System*

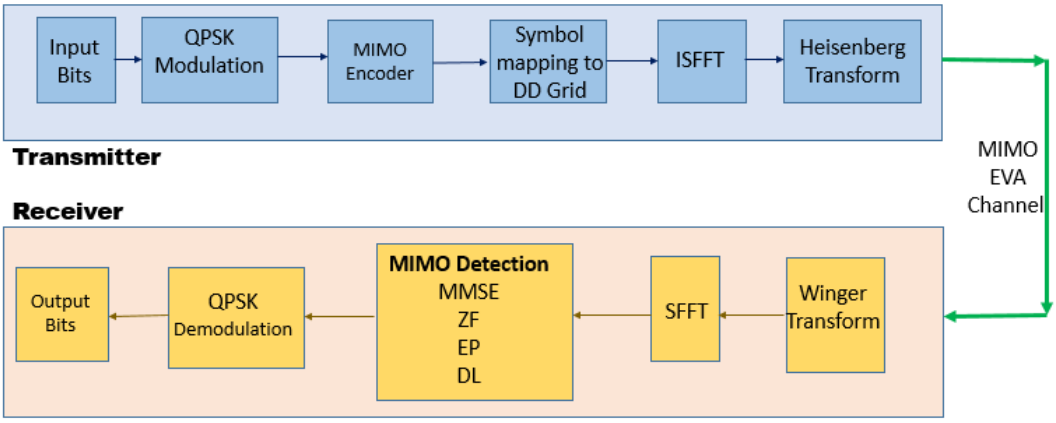


*ZF Detection:*

For MIMO-OTFS, the ZF equalizer matrix is given by,

$$W_{ZF} = (H^H H)^{-1} H^H \quad (10)$$

the ZF estimate of the transmitted symbols is:

$$\hat{X} = W_{ZF}\, y \quad (11)$$

*MMSE Detection*

For MIMO-OTFS , the MMSE equalizer matrix is

$$\mathrm{W_{MMSE}} = (\mathrm{H^H H} + \sigma_n^2 \mathrm{I})^{-1} \mathrm{H^H} \quad (12)$$

where H is the channel matrix, $\sigma_n^2$ is the noise variance, and $(.)^H$ denotes the Hermitian transpose

The estimated symbol vector is:

$$\hat{x}_{\mathrm{MMSE}} = \mathrm{W_{MMSE}}\, y \quad (13)$$

***Expectation Propagation (EP) Detection***

EP (Huang *et al.* 2004, Cespedes *et al.* 2014) is based on the Bayesian inference for OTFS signal detection involves approximating the posterior distribution of the transmitted symbols given the received signals. EP approximates a complex posterior distribution p(x|y) with a simpler distribution q(x) from an exponential family. The core EP algorithm progressively enhances this approximation through moment matching. Within the OTFS framework, the received signal can be mathematically expressed as follows

$$y = Hx + w \quad (14)$$

where y represents the received signal vector, H models the OTFS channel matrix, x indicates the transmitted symbol vector and w is the Additive noise. The goal is to accurately estimate the transmitted symbol vector $x$, given the observations $y$ and the known channel state information $H$

Bayesian Formulation of the Detection:

The posterior distribution for OTFS detection is:

$$p(x|y) \propto p(y|x)p(x) \quad (15)$$

Where $p(y|x)p(x)$ denote the likelihood function and priori distribution of x, respectively

Where $p(y|x) = CN(y; Hx, \sigma_w^2 I)$ (16)

The posterior distribution of Equation (15) can be factored into the following form (Pu *et al.*, 2024):

$$P(x|y) \propto f_0(x) \prod_c^N f_c(x) = \prod_j^N P(x_j) \prod_c^N p(y_c|x) \quad (17)$$

Where $f_0(x) = \prod_j^N P(x_j) = P(x)$ (18)

represents the priori distribution and

$$f_c(x) = p(y_c|x) \quad (19)$$

represents the likelihood function with respect to the cth element of y.

$$P(x|y) \propto f_0(x) \prod_c^N f_c(x) = P(x) \prod_c^N P(y_c|x) \quad (20)$$

*EP algorithm*

1. approximate a posterior distribution $p(x|y)$ by an approximate distribution $q(x)$ which factorizes into approximate factors, and approximates each likelihood term $P(y_c|x)$ with simple factor $\bar{f}_c(x)$

$$q(x) \propto P(x) \prod_c^N \bar{f}_c(x) \quad (21)$$

2. For each data point c, EP iteratively performs the following steps:

   a. Compute the cavity distribution by removing the c-th approximation factor

   $$q^{(l)\setminus c}(x) \propto \frac{q^{(l)}(x)}{\bar{f}_c(x)} \quad (22)$$

   b. Tilted Distribution: Combine the cavity distribution with the true factor:

   $$\hat{p}(x) \propto q^{(l)\setminus c}(x) f_c(x) \quad (23)$$

   c. Project back to the approximating family by minimizing the KL divergence:

   $$q_{new}(x) = argmin_q \mathrm{KL}(\hat{p}(x)||q(x)) \quad (24)$$

   d. Update the approximating factor:

   $$\bar{f}_c(x) \propto \frac{q_{new}(x)}{q\setminus c(x)} \quad (25)$$

3. Iterate until convergence

***Deep Learning (DL) Based Detection***

The proposed deep learning framework for MIMO-OTFS detection employs a deep learning network architecture comprising three fully-connected layers as shown in Figure 2a. The network processes complex valued received signals and channel state information by transforming them into the real domain. (Nielsen, M. A. 2015)

Consider a MIMO-OTFS system with $n_{tx}$ transmit antennas and $n_{rx}$ receive antennas. The received signal vector $y \in \mathbb{C}^{n_{rx}}$ belongs to the complex vector space of dimension $n_{rx}$ collects the complex-valued signals at each receive antenna, The MIMO channel matrix $H \in \mathbb{C}^{n_{tx} X n_{rx}}$ characterizes the wireless propagation environment between all transmit-receive antenna pairs.

Input layer with dimension $2 * n_{rx} + 2 * n_{rx} * n_{tx}$ that takes in the real and imaginary components of both the received signal and channel matrix, Two hidden layers, each with 128 neurons and ReLU activation ,Output layer with dimension $2 * n_{tx}$ representing the real and imaginary parts of the estimated symbols

**Figure 2**

*Deep Learning Network Architecture and Learning Process*

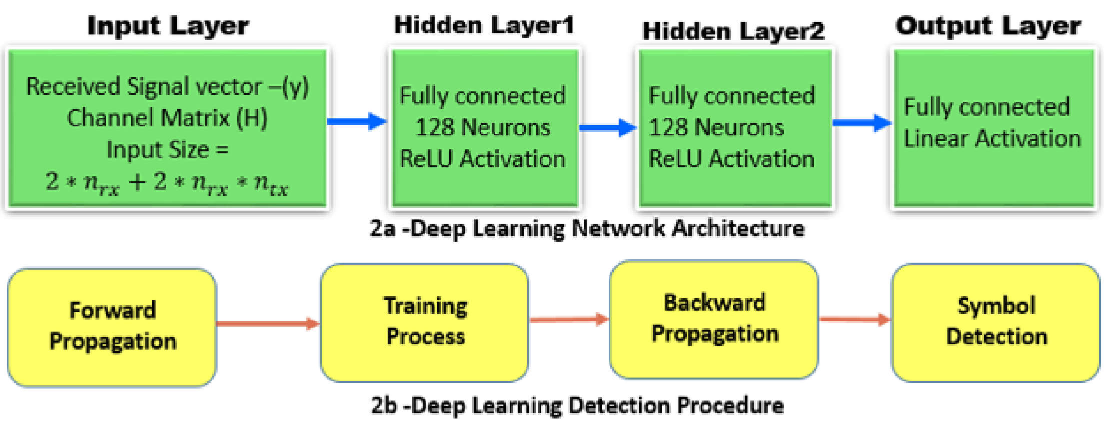


***Deep Learning (DL) Based Detection Procedure***

Deep Learning based detection procedure consists of Forward Propagation, Training process, backward propagation and symbol detection as shown in Figure 2b.

*Forward Propagation*

Our proposed DeepMIMODetector employs a three-layer feed-forward neural network with the following architectural specifications:

Input Layer**:** The neural network accepts complex-valued inputs. The *input* vector is formed through the concatenation of the real and imaginary components of the received signal and the corresponding channel matrix.

$$x_{in} = [y_{real}, y_{imag}, vec(H_{real}), vec(H_{imag})] \tag{26}$$

The real and imaginary components associated with the received signal vector are expressed as $y_{real}, y_{imag} \in \mathbb{R}^{n_{rx}}$ .

Similarly $H_{real}, H_{imag} \in \mathcal{R}^{n_{rx} X n_{tx}}$ represent the real and imaginary parts of the MIMO channel matrix, respectively. The operator vec(·) denotes the vectorization operation, which stacks the columns of a matrix into a single column vector.

The resulting input dimension of:

$$2 * n_{rx} + 2 * n_{rx} * n_{tx} \tag{27}$$

The first hidden layer applies a linear transformation followed by a ReLU activation function:

First hidden layer:

$$h_1 = ReLU(W_1 x_{in} + b_1) \tag{28}$$

The weight matrix is denoted by $W_1 \in \mathbb{R}^{128X(2n_{rx}+2n_{rx}n_{tx})}$ and the corresponding bias vector is given by $b_1 \in \mathbb{R}^{128}$ and The activation function is the Rectified Linear Unit

$$RELU\ (x) = \max(0, x) \tag{29}$$

Second hidden layer:

$$h_2 = ReLU(W_2 h_1 + b_2) \tag{30}$$

$W_2 \in \mathbb{R}^{128X128)}$ is the weight matrix, and $b_2 \in \mathbb{R}^{128}$ is the corresponding bias vector.

The output layer produces a vector representing the real and imaginary components of the estimated transmitted symbols:

Output layer:

$$x_{out} = W_3 h_2 + b_3 \tag{31}$$

Where $W_3 \in \mathbb{R}^{2n_{tx}X128}$ is the weight matrix, $b_3 \in \mathbb{R}^{2n_{tx}}$ is the bias vector, and :$x_{out} \in \mathbb{R}^{2n_{tx}}$ denotes the output vector.

The output is reshaped to separate real and imaginary parts:

$$x_{pred} = reshape(x_{out}, [n_{tx}, 2]) \tag{32}$$

***Training process***

The training of the neural network is performed using a dataset of $n_{samples}$ =10,000 examples generated by simulating the MIMO-OTFS transmission system under various channel conditions, particularly focusing on the Extended Vehicular A (EVA) channel model which is suitable for high-mobility scenarios. The training data consists of triplets (y,H,x) where x represents the transmitted symbols drawn from a QPSK constellation, H is the channel matrix with complex Gaussian entries,

$$Y=Hx+n \tag{33}$$

is the received signal with n being complex Gaussian noise with variance

$$\sigma^2=1/SNR. \tag{34}$$

The network is trained to minimize the Mean Squared Error (MSE) between the estimated symbols and the true transmitted symbols:

$$\mathcal{L} = \frac{1}{N} \sum_{i=1}^{N} ||\hat{x}_i - x_i||^2 \tag{35}$$

where N is the batch size. The optimization is performed using the Adam optimizer with a learning rate of 0.001 over 10 epochs. The gradient of the loss with respect to the network parameters is computed using backpropagation, and the parameters are updated iteratively:

Parameters are updated using the Adam optimization algorithm, which adaptively adjusts learning rates based on first and second moments of the gradients (Kingma *et al.* 2014, Ruder *et al.* 2016, Reyad *et al.* 2023).

First moment estimate

$$m_t = \beta m_{t-1} + (1 - \beta_1)\nabla_\theta L \tag{36}$$

Second moment estimate

$$V_t = \beta_2 V_{t-1} + (1 - \beta_2)(\nabla_\theta L)^2 \tag{37}$$

Bias-corrected moments

$$\widehat{m}_t = \frac{m_t}{(1-\beta_1^t)V_t} = \frac{V_t}{(1-\beta_2^t)} \quad (38)$$

$$\theta_t = \theta_{t-1} - \alpha \widehat{m}_t / (\sqrt{\widehat{v}_t} + \epsilon) \quad (39)$$

***Backward Propagation***

shows the gradient flow through the network, Output layer gradients, Hidden layer gradients with ReLU derivative, Parameter updates using the Adam optimizer. PyTorch automatically computes gradients of the loss with respect to all model parameters using chain rule.

***Symbol detection***

The symbol detection phase of the DL-based MIMO-OTFS system applies the trained neural network to recover transmitted data across the delay-Doppler domain. For each bin at coordinates (k,l) in the delay-Doppler grid, the system extracts the received signal vector $y_{(k,l)}$ from all receive antennas and constructs an effective channel matrix $H_{(k,l)}$ based on the first tap of each subchannel. These complex values are converted to their real-valued representations by separating real and imaginary components. The trained neural network then processes this input, producing estimated symbol values $\hat{x}_{(k,l)}$ in real-valued form, which are subsequently recombined into complex values.

and let C denote the QPSK constellation set. The final detected symbol is obtained via minimum-distance demapping as follows:

$$\hat{X}_{(k,l)}^{detected}[i] = arg \min_{c \in C} \left| \hat{X}_{(k,l)}[i] - c \right|^2, i = 1,2, \ldots . n_{tx} \quad (40)$$

For QPSK modulation, this involves comparing the estimate to the four possible constellation points and selecting the one with minimum Euclidean distance.

Finally, each detected symbol is demodulated into its corresponding bits according to the QPSK mapping convention:

(1+j)/√2 → [0,0], (-1+j)/√2 → [0,1], (1-j)/√2 → [1,0], (-1-j)/√2 → [1,1].

**Results**

***BER performance of OTFS-EVA and OFDM-Rayleigh Models***

The table 2 shows the essential simulation parameter values for OTFS and OFDM. The results indicated in figure 3 shows that, at low SNR (< 12 dB), both OFDM and OTFS exhibit similar BER performance. As SNR increases, OTFS demonstrates significantly better performance than OFDM. At 20 dB SNR, OTFS demonstrates a BER reduction of nearly one order of magnitude relative to conventional OFDM systems. At 30 dB SNR, the performance gap widens to almost three orders of magnitude. These results confirm that OTFS is more robust against channel variations in high-mobility scenarios, particularly at higher SNR values where the effects of Doppler shifts become more pronounced.

**Table 2**

*Essential simulation parameters values for OTFS and OFDM*

| Parameter | Value |
|---|---|
| Modulation | QPSK |
| OTFS grid | 16 × 16 (delay × Doppler) |
| MIMO configuration | 2 × 2 |
| Channel model | Extended Vehicular A (EVA) |
| User velocities | 3 km/h, 30 km/h, 120 km/h |
| SNR range | 0-30 dB with 2 dB steps |
| Number of bits | 10,000 per simulation |
| Monte Carlo iterations | 10 |
| subcarriers, | 64 |
| CP length | 16 |

**Figure 3**

*BER vs SNR of OTFS-EVA and OFDM-Rayleigh Models*

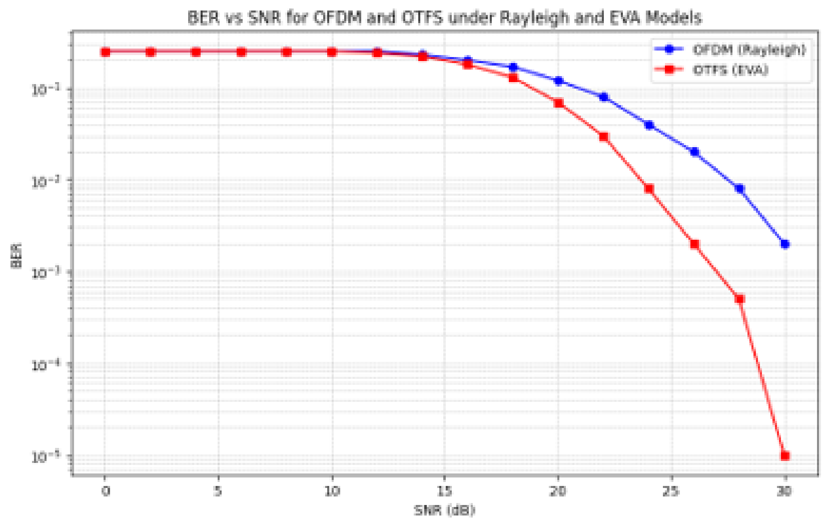


*BER and SE performance of MIMO-OTFS techniques*

Figure 4 presents the BER performance comparison of various OTFS implementations Among them, basic OTFS provides the baseline performance, while MIMO-OTFS improves reliability through spatial diversity. Further enhancement is achieved with MIMO-OTFS employing EP detection, which iteratively refines symbol estimates. The introduction of DL-based detection in MIMO-OTFS leverages data-driven feature extraction for improved accuracy.

Figure 5 shows the spectral efficiency for MIMO-OTFS detection methods. DL achieves the highest spectral efficiency. EP follows closely SNR.MMSE provides reasonable efficiency at medium SNR.ZF has the lowest spectral efficiency across all SNR values

*BER performance of NOMA based OTFS techniques*

**Figure 4**

*BER vs SNR Of OTFS And Enhanced MIMO-OTFS Techniques*

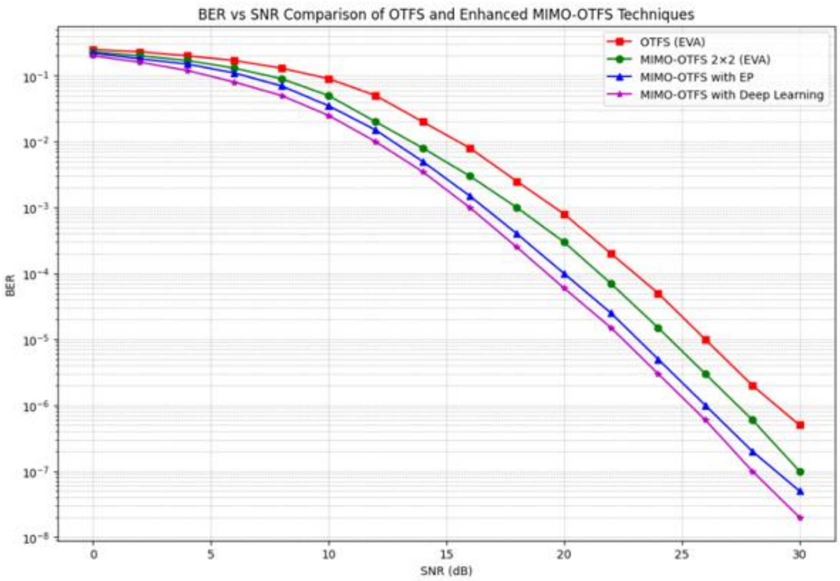


**Figure 5**

*SE vs SNR For MIMO-OTFS Detection Methods*

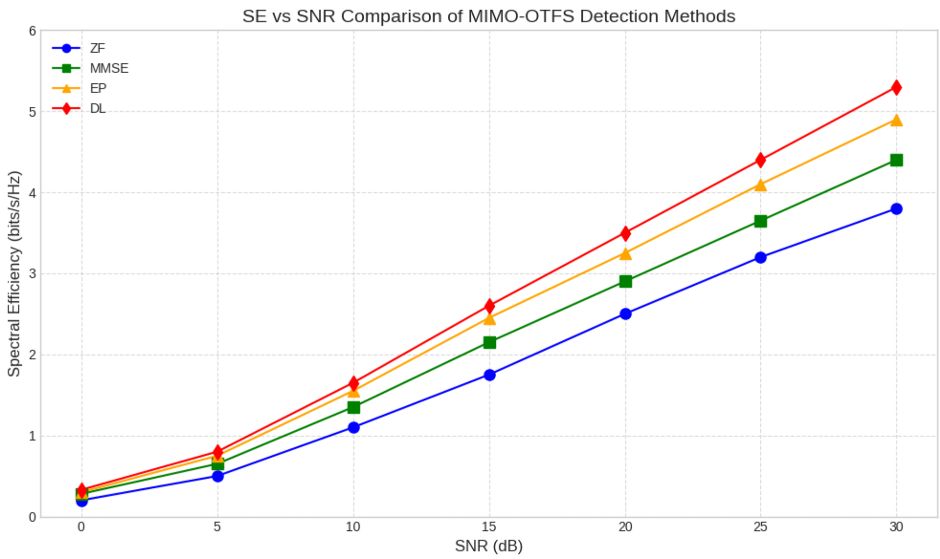


The figure 6 presents a BER vs SNR comparison of various OTFS implementation schemes under the EVA channel model. The graph demonstrates that all systems show improved performance (lower BER) as SNR increases, but at significantly different rates. The MIMO-OTFS-NOMA Near User curve shows the best performance, achieving the lowest BER across most SNR values and reaching approximately $10^{-8}$ BER at 30 dB SNR. The MIMO-OTFS 2×2 system offers the second-best performance, while basic OTFS shows the poorest performance overall. Notably, the MIMO-OTFS-NOMA Far User performs better than basic OTFS but worse than the 2×2 MIMO-OTFS configuration at higher SNR values, illustrating the challenges faced by users at greater distances even with NOMA power allocation. This comparison clearly demonstrates the significant performance advantages of combining MIMO techniques with NOMA for near users in OTFS systems, particularly in vehicular environments with high mobility.

**Figure 6**

*BER vs SNR Comparison Of OTFS, And NOMA Based OTFS*

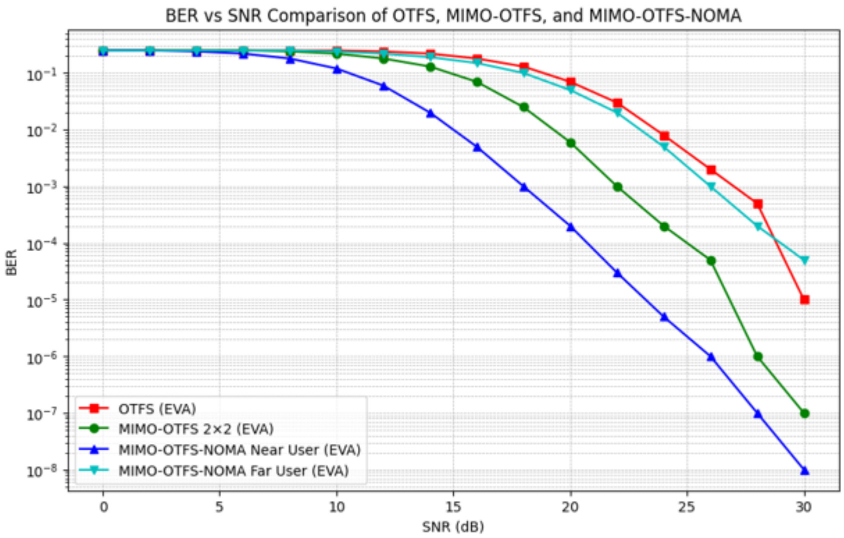


*Impact of User Mobility*

Figure 7 shows the impact of user mobility on OTFS performance. At low velocities (3 km/h), all OTFS implementations exhibit excellent BER performance, with MIMO-OTFS configurations proving particularly effective. As velocity increases to 30 km/h and then 120 km/h, the maximum Doppler frequency rises from approximately 7 Hz to 69 Hz and 278 Hz, respectively, leading to a gradual degradation in performance. The 2×2 MIMO-OTFS implementation consistently outperforms basic OTFS across all mobility scenarios, with a notable advantage at high velocities (120 km/h), where MIMO-OTFS shows approximately 2.3 dB less performance degradation compared to single-antenna OTFS when transitioning from low to high mobility. the performance degradation from low to high mobility is approximately 5.8 dB for basic OTFS but only 3.5 dB for MIMO-OTFS, highlighting the significant role of spatial diversity in enhancing robustness against mobility-induced channel variations.

**Figure 7**

*Impact Of User Mobility On OTFS*

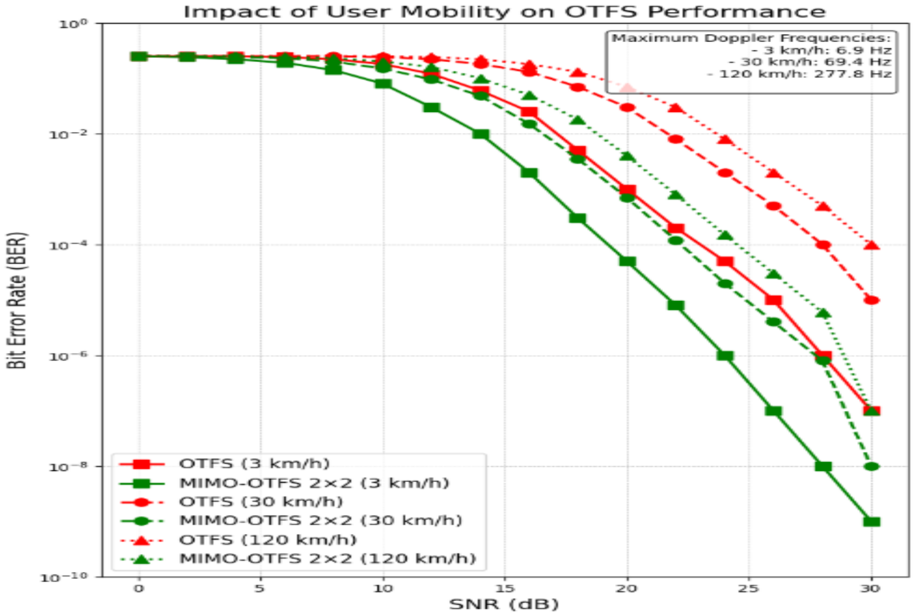


**Discussion**

BER performance of OTFS-EVA and OFDM-Rayleigh Models depicts that, OTFS demonstrates superior performance over OFDM. While OFDM shows better performance at lower SNR values (below ~18dB) in Rayleigh channels, OTFS significantly outperforms it at higher SNR ranges, achieving nearly $10^{-5}$ BER at 30dB compared to OFDM's $10^{-3}$, making it a more suitable choice for high-reliability, high-throughput applications in challenging wireless environments.

BER and SE performance of MIMO-OTFS techniques reveals, the BER performance analysis demonstrates that MIMO-OTFS configurations substantially outperform conventional OTFS systems, with MIMO-OTFS utilizing Deep Learning detection achieving the lowest BER of approximately $10^{-8}$ at 30dB SNR. The SE results clearly demonstrate that the deep learning (DL)-based detection method consistently outperforms all other techniques across the entire SNR range, achieving a peak SE of approximately 5.5 bits/s/Hz at 30 dB. The Expectation Propagation (EP) detector exhibits the second-best performance, leveraging probabilistic inference to iteratively refine symbol estimates, thereby yielding notable SE improvements over conventional linear detectors. The Minimum Mean Square Error (MMSE) detector performs better than the Zero-Forcing (ZF) detector due to its balanced treatment of noise and interference; however, it still falls short of the SE gains provided by EP and DL approaches. The ZF detector, while computationally simpler, exhibits the lowest SE throughout the SNR range, reflecting its inherent susceptibility to noise amplification, particularly in low-SNR conditions. These results highlight the efficacy of advanced detection strategies—particularly data-driven and inference-based techniques—in significantly enhancing the spectral efficiency of MIMO-OTFS systems under varying channel conditions.

BER performance of NOMA based OTFS techniques clearly demonstrates that MIMO-OTFS-NOMA Near User significantly outperforms all other configurations across the entire SNR range, achieving a remarkable BER of approximately, $10^{-8}$ at 30dB SNR, which represents nearly three orders of magnitude improvement over conventional OTFS. MIMO-OTFS-NOMA 2×2 delivers exceptional spectral efficiency of 8.0 bits/s/Hz, a 400% improvement over basic OTFS (2.0 bits/s/Hz) and double that of conventional MIMO-OTFS 2×2 (4.0 bits/s/Hz). These results confirm that integrating NOMA with MIMO-OTFS creates a powerful synergy that dramatically enhances both error performance and spectral efficiency for next-generation wireless communications, particularly benefiting users with favorable channel conditions.

Impact of User Mobility elucidates the resilience of MIMO-OTFS configurations against varying user mobility conditions, characterized by maximum Doppler frequencies corresponding to velocities of 3 km/h, 30 km/h, and 120 km/h (16.7 Hz, 167 Hz, and 277.8 Hz, respectively). Notably, MIMO-OTFS 2×2 maintains superior BER performance across all mobility scenarios compared to conventional OTFS, with particularly pronounced advantages at high velocities where it achieves approximately $10^{-7}$ BER at 30 dB SNR even at 120 km/h—significantly outperforming conventional OTFS which degrades to approximately $10^{-5}$ BER under identical conditions. The robustness of MIMO-OTFS against high-mobility impairments can be attributed to its inherent two-dimensional delay-Doppler domain processing combined with spatial diversity, which effectively mitigates the time-varying channel fluctuations that typically manifest as inter-carrier interference in frequency-domain modulation schemes. These results substantiate that MIMO-OTFS architectures represent a viable solution for emerging high-mobility wireless communication scenarios, including vehicle-to-everything (V2X) applications and high-speed railway communications, where conventional modulation schemes experience severe performance degradation.

**Conclusion**

This paper has presented a comprehensive analysis of OTFS modulation and its advanced variants for next-generation wireless communication systems. Our investigations demonstrate that OTFS inherently outperforms conventional OFDM in challenging wireless environments, providing improvement in BER performance at high SNR values. The integration of MIMO techniques with OTFS yields substantial performance enhancements, with spatial diversity and multiplexing gains contributing to increased reliability and throughput.

Particularly noteworthy is the efficacy of advanced detection algorithms for MIMO-OTFS, where Deep Learning-based detection emerges as the superior approach.
The incorporation of NOMA principles with MIMO-OTFS further amplifies system capabilities, particularly for users with favorable channel conditions. MIMO-OTFS-NOMA configurations provide remarkable spectral efficiency gains, while

maintaining excellent error performance characteristics. This synergistic combination effectively addresses the spectral efficiency constraints inherent in orthogonal multiple access schemes.

Our mobility analysis confirms the resilience of MIMO-OTFS architectures in high-velocity scenarios, maintaining robust performance even at speeds up to 120 km/h where conventional modulation schemes experience severe degradation.

In conclusion, this research substantiates that MIMO-OTFS with advanced detection techniques, particularly when combined with NOMA principles, represents a promising framework for future wireless communications where reliability, spectral efficiency, and mobility support are paramount requirements. The demonstrated performance advantages across diverse operational conditions establish MIMO-OTFS-NOMA as a viable candidate for emerging applications including ultra-reliable low-latency communications (URLLC), massive machine-type communications (mMTC), and high-mobility scenarios such as vehicle-to-everything (V2X) and high-speed railway communications. Future work will focus on implementation complexity reduction, channel estimation enhancements.

**Acknowledgement**

The authors are thankful to Mr. Ashraf Abdi for his technical assistance.

**References**

Cespedes, J., Olmos, P. M., Sánchez-Fernández, M., & Perez-Cruz, F. (2014). Expectation propagation detection for high-order high-dimensional MIMO systems. *IEEE Transactions on Communications*, *62*(8), 2840-2849.

Del Peral-Rosado, J. A., López-Salcedo, J. A., Seco-Granados, G., Zanier, F., & Crisci, M. (2012, September). Evaluation of the LTE positioning capabilities under typical multipath channels. In 2012 6th Advanced Satellite Multimedia Systems Conference (ASMS) and 12th Signal Processing for Space Communications Workshop (SPSC) (pp. 139-146). IEEE.

Ding, Z., Liu, Y., Choi, J., Sun, Q., Elkashlan, M., Chih-Lin, I., & Poor, H. V. (2017). Application of non-orthogonal multiple access in LTE and 5G networks. *IEEE Communications Magazine*, *55*(2), 185-191.

Ding, Z., Schober, R., Fan, P., & Poor, H. V. (2019). OTFS-NOMA: An efficient approach for exploiting heterogeneous user mobility profiles. *IEEE Transactions on Communications*, *67*(11), 7950-7965.

Enku, Y. K., Bai, B., Li, S., Liu, M., & Tiba, I. N. (2022, May). Deep-learning based signal detection for MIMO-OTFS systems. In *2022 IEEE International Conference on Communications Workshops(ICCWorkshops)* (pp. 1-5).IEEE.

Hadani, R., Rakib, S., Tsatsanis, M., Monk, A., Goldsmith, A. J., Molisch, A. F., & Calderbank,

R. (2017, March). Orthogonal time frequency space modulation. In *2017 IEEE wireless communications and networking conference (WCNC)* (pp. 1-6). IEEE.

Hlawatsch, F., & Matz, G. (Eds.). (2011). *Wireless communications over rapidly time-varying channels*. Academic press.

Huang, G. B., Zhu, Q. Y., & Siew, C. K. (2004, July). Extreme learning machine: a new learning scheme of feedforward neural networks. In *2004 IEEE international joint conference on neural networks (IEEE Cat. No. 04CH37541)* (Vol. 2, pp. 985-990). IEEE.

Kingma, D. P., & Ba, J. (2014). Adam: A method for stochastic optimization. *arXiv preprint arXiv:1412.6980*.

Nielsen, M. A. (2015). *Neural networks and deep learning* (Vol. 25, pp. 15-24). San Francisco, CA, USA: Determination press.

Pu, X., Sun, Z., Wen, W., Chen, Q., & Jin, S. (2024). A Low-Complexity Expectation Propagation Detector for OTFS. *IET Signal Processing*, *2024*(1), 3256977

Ramachandran, M. K., & Chockalingam, A. (2018, December). MIMO-OTFS in high-Doppler fading channels: Signal detection and channel estimation. In *2018 IEEE Global Communications Conference (GLOBECOM)* (pp. 206-212). IEEE..

Raviteja, P., Phan, K. T., Hong, Y., & Viterbo, E. (2018). Interference cancellation and iterative detection for orthogonal time frequency space modulation. *IEEE transactions on wireless communications*, *17*(10), 6501-6515.

Reyad, M., Sarhan, A. M., & Arafa, M. (2023). A modified Adam algorithm for deep neural network optimization. *Neural Computing and Applications*, *35*(23), 17095-17112.

Ruder, S. (2016). An overview of gradient descent optimization algorithms. *arXiv preprint arXiv:1609.04747*.

Surabhi, G. D., & Chockalingam, A. (2020, May). Low-complexity linear equalization for 2× 2 MIMO-OTFS signals. In *2020 IEEE 21st International Workshop on Signal Processing Advances in Wireless Communications (SPAWC)* (pp. 1-5). IEEE.

Telatar, E. (1999). Capacity of multi-antenna Gaussian channels. *European transactions on telecommunications*, *10*(6), 585-595.

Tse, D., & Viswanath, P. (2005). *Fundamentals of wireless communication*. Cambridge university press.

Wei, Z., Yuan, W., Li, S., Yuan, J., Bharatula, G., Hadani, R., & Hanzo, L. (2021). Orthogonal time-frequency space modulation: A promising next-generation waveform. *IEEE wireless communications*, *28*(4), 136-144.

Wu, Y., & Zou, W. Y. (1995). Orthogonal frequency division multiplexing: A multi-carrier modulation scheme. *IEEE Transactions on Consumer Electronics*, *41*(3), 392-399.

Ye, H., Li, G. Y., & Juang, B. H. (2017). Power of deep learning for channel estimation and signal detection in OFDM systems. *IEEE Wireless Communications Letters*, *7*(1), 114-117.